Band structure and associated electromagnetic fields in one-dimensional photonic crystals with left-handed materials

M. de Dios-Leyva and O. E. González-Vasquez
Department of Theoretical Physics, University of Havana, San Lázaro y L, Vedado 10400, Havana, Cuba
(Received 18 June 2007; revised manuscript received 12 September 2007; published 4 March 2008)

We have investigated, for oblique propagation, the dispersion relation and associated electric fields of one-dimensional photonic crystals composed of alternating layers of right-handed and left-handed materials (RHM and LHM). Calculations are performed by assuming that the dielectric permittivity and magnetic permeability are constant in the RHM, whereas both parameters follow a plasmalike dispersion in the LHM. It is shown that the dispersion curves and associated electric fields exhibit, as functions of the propagation angle θ, interesting features around both the magnetic plasma frequency ω_m and the frequency ω_0 at which the spatial average of the wave vector component perpendicular to the layers $\bar{Q}$ vanishes. The features around ω_m are determined by the occurrence of a strong coupling between the radiation field and the "magnetic plasma" contained in the LHM, for $\theta \neq 0$. The higher band associated with the coupled modes as well as the lower one exhibit a plasmonlike behavior when ω is close to ω_m, whereas the former band exhibits a photonlike behavior for higher frequencies. Around ω_0, a zero-$\bar{Q}$ gap opens, and its properties, as functions of the propagation angle θ, depend on the geometrical and physical parameters of the constituents. It is shown that the photonic-band inversion phenomenon can occur in the considered structure, which can also exhibit a zero-$\bar{Q}$ gap of zero width.

DOI: 10.1103/PhysRevB.77.125102 PACS number(s): 42.70.Qs, 78.20.Ci, 41.20.Jb

I. INTRODUCTION

Since the experimental realization of composite metamaterials[1–3] exhibiting both negative dielectric permittivity $\varepsilon(\omega)$ and negative magnetic permeability $\mu(\omega)$ in some frequency ranges, a great deal of attention has been paid to the study of the electromagnetic properties of these photonic structures. This is due to the interesting basic physical properties of these materials and to their potential technological applications in a wide range of optical devices. A medium of this type, which also exhibits a negative index of refraction, $n=\sqrt{\varepsilon(\omega)}\sqrt{\mu(\omega)}$, is called left-handed material (LHM) because for an electromagnetic plane wave propagating in it, the corresponding wave vector $\vec{k}$, electric field $\vec{E}$, and magnetic field $\vec{H}$ form a left-handed orthogonal set,[4] contrary to all known naturally occurring materials where the triplet of these vectors is right handed. These metamaterials are necessarily dispersive and the existence of some frequency ranges where their material parameters are negative is closely associated with resonance phenomena. The rapidly growing interest in left-handed materials,[5] also called negative refractive materials, stems from their unusual physical properties, some of which, such as an inverse Snell's law, reversed Doppler and Cherenkov effects, and a Poynting vector directed opposite to the wave vector $\vec{k}$, were discussed 40 years ago by Veselago.[4] It should be pointed out that one of the most important concepts associated with the possible applications of LHMs is the concept of a perfect lens, which can focus both propagating and evanescent waves and provide a perfect image of a point source. The use of a LHM slab as a perfect lens was suggested by Pendry in 2000,[6] who also showed that the role of the surface plasmons[7] is crucial to the action of such an optical device.

Recent interest in these metamaterials has been directed toward the study of one-dimensional (1D) photonic structures composed of alternating layers of homogeneous LHM and right-handed material (RHM). It has been shown[8–13] that such layered structures exhibit new types of electromagnetic properties that do not exist in ordinary structures constituted only of RHM. Li *et al.*[8] showed the existence of a new type of band gap in RHM-LHM-photonic crystals that corresponds to the frequency at which the spatial average of the refractive index, taken over a period of the 1D photonic structure, vanishes. These authors suggested that, in contrast to the Bragg gap, such a zero-$\bar{n}$ gap is insensitive to the geometrical scaling of the structure and, possibly, structural disorder. This surprising result, established for the case of normal incidence, immediately directed a lot of attention toward the general study of the band structure of such periodic structures and the mentioned band gap, in particular. So, phenomena such as discrete and photon tunneling modes,[9] bands that originate from localized modes,[10] omnidirectional band gap,[11–13] etc., have been discussed by using different dependences of $\varepsilon(\omega)$ and $\mu(\omega)$ on ω for the LHM component, including the case where these physical parameters are frequency independent.[9,10] In particular, by using a plasmalike dispersion for both $\varepsilon(\omega)$ and $\mu(\omega)$, Jiang *et al.*[11] studied the angular dependence of the band structure for a RHM-LHM-photonic crystal and identified an omnidirectional band gap associated with the $\bar{n}=0$ condition for both TE and TH polarizations. These properties are not necessarily exhibited by other photonic crystals because, as shown by Daninthe *et al.*,[12] the $\bar{n}=0$ condition does not guarantee, in general, the existence of an angle insensitive omnigap for either or both polarizations.

As mentioned above, metamaterials are very dispersive, and negative values of their physical parameters $\varepsilon(\omega)$ and $\mu(\omega)$ originate from resonance.[14] This means that when the frequency ω of an electromagnetic field is near the corresponding resonance frequency, the interaction between the

radiation field and the RHM-LHM-photonic crystal may be strong enough, and the wave inside the medium must correspond to a coupled mode having contributions of the combined system.[15] The fact that such a coupling can affect the propagation of the radiation field in a very profound manner and may give rise to some new interesting effects has motivated us to study theoretically this phenomenon, which, up to now, has not received special attention. Here, a detailed study of the zero-$\bar{n}$ gap is also presented. The paper is organized as follows. In Sec. II, we detail the theoretical approach. Section III is concerned with the results and discussion. Finally, our conclusions are given in Sec. IV.

II. THEORETICAL FRAMEWORK

Here, we are concerned with a 1D photonic crystal consisting of alternating layers of materials A and B with permittivity and permeability given by (ε_1,μ_1) and (ε_2,μ_2), respectively. In general, these optical parameters are frequency-dependent functions but, for simplicity, we omit the explicit dependence in the notation. We choose x to represent the lateral direction, and z the stacking direction. The origin of coordinates is taken at the center of a first A layer. The structure has a lattice constant $d=a+b$, where a and b are the widths of layers A and B, respectively.

Let us consider a monochromatic electromagnetic wave propagating in the (x,z) plane with wave vector component q along the x axis, i.e., parallel to the layers. Under these conditions, the solutions of Maxwell's equations for TE polarization can be written down as

$$\vec{E}(\vec{r}) = \hat{y}E(z)\exp(iqx), \tag{1}$$

$$\frac{i\omega}{c}\mu(z)\vec{H}(\vec{r}) = \exp(iqx)\left[-\hat{x}\frac{dE(z)}{dz} + iq\hat{z}E(z)\right], \tag{2}$$

where $\vec{E}(\vec{r})$ and $\vec{H}(\vec{r})$ are the spatial parts of the electric and magnetic fields, respectively, and $E(z)$ satisfies the equation

$$-\frac{1}{\varepsilon(z)}\frac{d}{dz}\left[\frac{1}{\mu(z)}\frac{dE(z)}{dz}\right] + \frac{q^2}{\varepsilon(z)\mu(z)}E(z) = \frac{\omega^2}{c^2}E(z). \tag{3}$$

Similar solutions can be written for the TM-polarized electromagnetic fields. As for such modes the magnetic field may be taken as $\vec{H}(\vec{r})=\hat{y}H(z)\exp(iqx)$, it is not difficult to see that $H(z)$ satisfies Eq. (3) by interchanging the material parameters $\varepsilon(z)$ and $\mu(z)$, and the electric field $\vec{E}(\vec{r})$ is obtained from Eq. (2) making the substitutions $\vec{H}(\vec{r})\to\vec{E}(\vec{r})$, $E(z)\to H(z)$, and $\mu(z)\to-\varepsilon(z)$.

In order to obtain the dispersion relation of the considered photonic crystal and the corresponding expressions for the electromagnetic fields, it is convenient to use the transfer-matrix method utilized in Ref. 16 to study the electronic states in semiconductor superlattices and used in Ref. 17 to analyze the electromagnetic modes for the case of normal propagation ($q=0$). The usefulness of such a method is due to the fact that all the properties of the system, such as the photonic-band structure, symmetry of the different modes and its connection with the dispersion relation, existence of zero photonic-band gap, etc., are completely determined by the following frequency-dependent functions (for TE modes):

$$p(\omega) = \cos\frac{aQ_1}{2}\cos\frac{bQ_2}{2} - \frac{\mu_2}{\mu_1}\frac{Q_1}{Q_2}\sin\frac{aQ_1}{2}\sin\frac{bQ_2}{2}, \tag{4}$$

$$q(\omega) = \sin\frac{aQ_1}{2}\cos\frac{bQ_2}{2} + \frac{\mu_2}{\mu_1}\frac{Q_1}{Q_2}\cos\frac{aQ_1}{2}\sin\frac{bQ_2}{2}, \tag{5}$$

$$r(\omega) = \sin\frac{aQ_1}{2}\cos\frac{bQ_2}{2} + \frac{\mu_1}{\mu_2}\frac{Q_2}{Q_1}\cos\frac{aQ_1}{2}\sin\frac{bQ_2}{2}, \tag{6}$$

$$s(\omega) = \cos\frac{aQ_1}{2}\cos\frac{bQ_2}{2} - \frac{\mu_1}{\mu_2}\frac{Q_2}{Q_1}\sin\frac{aQ_1}{2}\sin\frac{bQ_2}{2}, \tag{7}$$

where

$$\text{(a) } Q_1 = \sqrt{\frac{\omega^2}{c^2}n_1^2 - q^2} \quad \text{and (b) } Q_2 = \sqrt{\frac{\omega^2}{c^2}n_2^2 - q^2}, \tag{8}$$

$n_i=\sqrt{\varepsilon_i}\sqrt{\mu_i}$, with $i=1,2$.

In fact, the transfer-matrix approach[16] allows us to write the dispersion relation in the following equivalent forms:

$$\cos^2\left(\frac{kd}{2}\right) = p(\omega)s(\omega), \tag{9}$$

$$\sin^2\left(\frac{kd}{2}\right) = q(\omega)r(\omega), \tag{10}$$

where k is the Bloch wave vector along the axis of the photonic crystal that relates the field in two consecutive unit cells by the factor $\exp(ikd)$ and is limited to the first Brillouin zone $-\pi/d<k<\pi/d$. The corresponding expressions for the electric field in the first unit cell can also be written in the following equivalent forms (see the Appendix):

$$\frac{E(z)}{E_0} = \cos Q_1 z + \frac{i\sin kd}{2q(\omega)s(\omega)}\sin Q_1 z \quad \text{for } |z| < \frac{a}{2}, \tag{11}$$

$$\frac{E(z)}{E_0} = \left[p(\omega) + \frac{i\sin kd}{2s(\omega)}\right]\cos Q_2\left(z-\frac{d}{2}\right) - \frac{\mu_2}{\mu_1}\frac{Q_1}{Q_2} \times\left[r(\omega) - \frac{i\sin kd}{2q(\omega)}\right]\sin Q_2\left(z-\frac{d}{2}\right) \quad \text{for } \frac{a}{2} < z < \frac{a}{2}+b, \tag{12}$$

and

$$\frac{E(z)}{E_1} = \frac{1}{dQ_1}\left[\sin Q_1 z - \frac{i\sin kd}{2p(\omega)r(\omega)}\cos Q_1 z\right] \quad \text{for } |z| < \frac{a}{2}, \tag{13}$$

$$\frac{E(z)}{E_1} = \frac{1}{dQ_1}\left\{\left[q(\omega) - \frac{i\sin kd}{2r(\omega)}\right]\cos Q_2\left(z - \frac{d}{2}\right) + \frac{\mu_2}{\mu_1}\frac{Q_1}{Q_2} \times \left[s(\omega) + \frac{i\sin kd}{2p(\omega)}\right]\sin Q_2\left(z - \frac{d}{2}\right)\right\} \quad \text{for } \frac{a}{2} < z < \frac{a}{2} + b, \tag{14}$$

where $E_0 = E(0)$ and $E_1 = \mu_1 d\left[\frac{1}{\mu}\frac{dE(z)}{dz}\right]_{z=0}$.

Of course, the electric fields in other elementary cells are determined by the Bloch condition $E(z+nd) = \exp(inkd)E(z)$. Furthermore, if we now use the fact that Eqs. (11)–(14) describe the same distribution of electric field throughout the structure, it is not difficult to obtain the following relation between the absolute square of E_0 and E_1:

$$\left|\frac{E_1}{E_0}\right|^2 = |(dQ_1)^2 F(\omega)|, \tag{15}$$

with

$$F(\omega) = p(\omega)r(\omega)/s(\omega)q(\omega). \tag{16}$$

The function $F(\omega)$, defined in Eq. (16), is independent of the Bloch wave vector k and may be used to study the properties of the electromagnetic modes and photonic bands at $k=0$ and $k=\pm\pi/d$. In fact, the zeros and singularities of $F(\omega)$ are directly related to the symmetry properties of the electromagnetic modes and to the frequencies of the photonic bands at these points. This follows immediately from Eqs. (9)–(15) by noting that at $k=0(k=\pm\pi/d)$, the electromagnetic modes are even functions of z when $r(\omega)=0[p(\omega)=0]$ and $q(\omega)\neq 0[s(\omega)\neq 0]$, whereas they are odd functions of z when $r(\omega)\neq 0[p(\omega)\neq 0]$ and $q(\omega)=0[s(\omega)=0]$. So, from a plot of $F(\omega)$ as a function of ω, for a particular choice of the geometrical and physical parameters, one can immediately know the symmetry distribution of modes and the corresponding frequencies at $k=0$ and $k=\pm\pi/d$. Due to this, $F(\omega)$ has been systematically used to verify and control the numerical calculations presented below.

We stress that the formulas presented above are general enough and may be used to study the oblique propagation of TE and TM electromagnetic modes in photonic crystals composed of two different materials A and B with all sorts of permittivity and permeability (refractive index) configurations. Of course, they can also be used to obtain equations describing the TE and TM modes in structures which may be considered as limiting cases of the photonic crystal when appropriate limits for the layer widths a and b are taken. As examples of such limiting structures, we can mention a medium composed of two semi-infinite materials separated by a flat interface, and a layer embedded between two semi-infinite identical materials. Works devoted to the study of interface and confined modes in these structures have been reported recently.[10,18]

Finally, it should be pointed out that the $\bar{n}=0$ condition, which guarantees the existence of a zero-$\bar{n}$ gap in a RHM-LHM-photonic crystal for normal propagation ($q=0$), must be conveniently extended[19] in order to treat the case of oblique propagation ($q\neq 0$). In fact, it is not difficult to see from Eq. (10) that such a condition takes the form

$$\bar{Q}(\omega_0) = \frac{1}{d}\int_0^d Q(z,\omega_0)dz = \frac{1}{d}[aQ_1 - bQ_2(\omega_0)] = 0. \tag{17}$$

This equation determines the frequency ω_0 at which the corresponding gap opens and at which the spatial average of the z-component Q [see Eq. (8)] of the wave vector, taken over a period of the photonic structure, vanishes. The presence of $-Q_2(\omega_0)$ in the right-hand side of Eq. (17) is associated with the fact that the wave vector of the electromagnetic field is oriented exactly opposite to the Poynting vector in the LHM, and its component q parallel to the layers is conserved throughout the structure. Of course, relation (17) reduces to the $\bar{n}=0$ condition for $q=0$.

III. RESULTS AND DISCUSSION

In what follows, we focus on photonic crystals consisting of alternating and homogeneous layers of medium A, characterized by positive and frequency independent parameters ε_1 and μ_1, and medium B with a plasmalike dispersion for the effective permittivity $\varepsilon_2(\omega)$ and permeability $\mu_2(\omega)$ given by[11]

$$\varepsilon_2(\omega) = \varepsilon_0 - \left(\frac{\omega_p}{\omega}\right)^2, \tag{18}$$

$$\mu_2(\omega) = \mu_0 - \left(\frac{\omega_m}{\omega}\right)^2, \tag{19}$$

where ε_0, μ_0, ω_p, and ω_m are positive constants and $\omega = 2\pi\nu$ is the angular frequency measured in gigahertz. This type of photonic structure can be experimentally realized by incorporating a composite made of periodically loaded medium (see Ref. 5 and references therein). These media have, in general, good microwave properties and exhibit large bandwidth, i.e., the frequency range where the effective permittivity $\varepsilon_2(\omega)$ and permeability $\mu_2(\omega)$ are both negative is relatively wide.

On the other hand, photonic crystals involving the LHM layer can also be experimentally realized at microwave frequency by incorporating metamaterials which are obtained by embedding in host media small inclusions of wires and split ring resonators (SRRs). These metamaterials are characterized by an effective permittivity following a plasmalike dispersion and an effective permeability following a Lorentz-type dispersion. They exhibit narrow bandwidths and considerable amount of loss in the microwave region. Some authors,[12,19] however, ignoring dissipation have studied the band gap structure of these RHM-LHM-photonic crystals, and some of their results reveal properties similar to those obtained (see below) when the LHM layer has $\varepsilon_2(\omega)$ and $\mu_2(\omega)$, following the plasmalike dispersion [Eqs. (18) and (19). The quantitative difference between these results is mainly determined by effects associated with the bandwidth. Based on these observations and in a first approximation, we

may consider the layer made of wire and SRR material modeled via the plasmalike dispersion [Eqs. (18) and (19)].

Furthermore, metamaterials based on other classes of small inclusions in host media such as broadside coupled SRRs, capacitively loaded strips and SRR, omega structures, and space-filling elements have also been proposed.[5] Almost all metamaterials are by their nature anisotropic. In the theoretical and experimental studies of these structured materials, the Lorentz model and the model for which both the effective permittivity and permeability follow a plasmalike dispersion (Drude model) have been used. As mentioned above, the difference between the results obtained by using the Lorentz model and those obtained when the Drude model is used is determined by the effects associated with the bandwidth. Taking such effects into account, some authors (see Ref. 20 and references therein) have preferred the Drude model because it provides a much wider bandwidth and allows to simplify the calculations. These observations illustrate the usefulness of the Drude model in the study of these structured materials.

Now, if it is supposed that $\varepsilon_0 > \mu_0$, then $\varepsilon_2(\omega)$ and $\mu_2(\omega)$ are both negative for $\omega < \omega_p/\sqrt{\varepsilon_0}$ (and medium B is a LHM in this frequency range), have opposite signs for $\omega_p/\sqrt{\varepsilon_0} < \omega < \omega_m/\sqrt{\mu_0}$, indicating an evanescent behavior in this frequency range, and are both positive for $\omega > \omega_m/\sqrt{\mu_0}$.

In order to perform the numerical calculations, we focus on the structure for which the constituting materials are air (layer A, with $\varepsilon_1=1$ and $\mu_1=1$) and a medium B with[11] $\varepsilon_0=1.21$, $\mu_0=1$, and $\omega_p=\omega_m=10$ GHz. Note that, for this multilayer structure, we can take $q=(n_1\omega/c)\sin\theta=(\omega/c)\sin\theta$, where θ is the propagation angle. This observation allows us to investigate the band structure and associated fields as functions of θ. As will be shown below, the choice of this photonic system allows us to know in detail the fundamental features of the zero-$\bar{n}$ gaps (or the zero-$\bar{Q}$ gaps) and of the coupled modes resulting from the interaction between the radiation field and the photonic crystal. Also, the present calculations may be compared with those of Jiang *et al.*[11] and Daninthe *et al.*,[12] who studied the angular dependence of the band gap for such photonic structure using specific values for the relevant physical parameters.

Now, due to the importance of the frequency $\nu_0=\omega_0/2\pi$ [see Eq. (17)] in the study of the considered photonic crystals, we present in Fig. 1 its dependence on the ratio a/b, for different values of the propagation angle θ, and on θ for various values of a/b. It follows from Fig. 1(a) that ν_0, for a fixed value of θ, is a decreasing function of the ratio a/b. However, its dependence on θ depends on the range of a/b considered. In fact, while ν_0 decreases with θ for $a/b<1$, it increases for $a/b>1$. It should be noted also that ν_0 is independent of θ for $a/b=1$. The latter result follows immediately from Eqs. (8) and (17) and is a direct consequence of the conservation of the wave vector component q parallel to the layers. Of course, this result must be also valid for any other RHM-LHM-photonic crystal for which the equation $\varepsilon_1\mu_1=\varepsilon_2(\omega)\mu_2(\omega)$ has a real solution.

Let us now consider the solutions of either Eq. (9) or (10). These solutions give the dispersion relation or photonic-band structure associated with the TE modes of the photonic crystal. As mentioned before, here, we focus on the photonic bands situated around and above the corresponding zero-$\bar{Q}$ gap, which are displayed in Figs. 2 and 3 for two values of the ratio a/b and different values of the propagation angle θ.

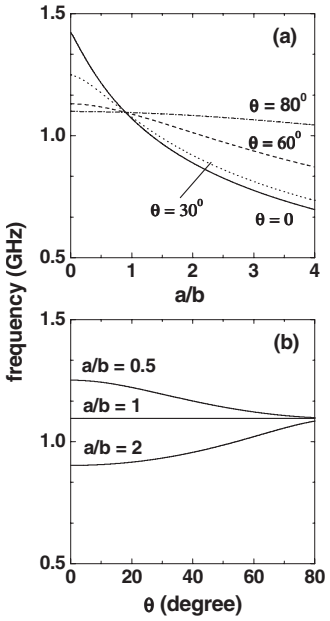

FIG. 1. Frequencies $\nu_0=\omega_0/2\pi$ at which $\bar{Q}=0$ as functions of (a) the ratio a/b for different values of the propagation angle θ and (b) the angle θ for various values of the ratio a/b.

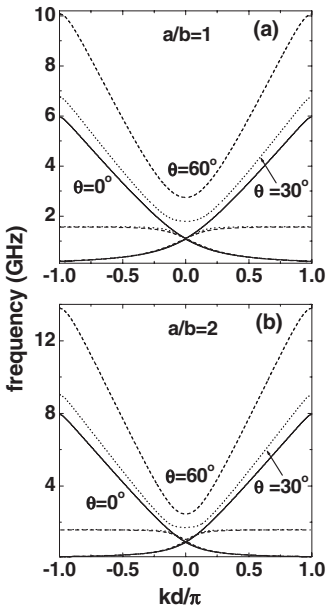

FIG. 2. Dispersion curves of the TE modes for a photonic crystal composed of alternating layers of air and a material B with $\varepsilon_2(\omega)$ and $\mu_2(\omega)$ given by Eqs. (18) and (19), respectively, for (a) $a/b=1$, with $a=12$ mm, and (b) $a/b=2$, with $a=12$ mm, and for different values of the propagation angle θ. The frequency $\nu=\omega/2\pi$ is presented as a function of the reduced Bloch wave vector $\tau=kd/\pi$.

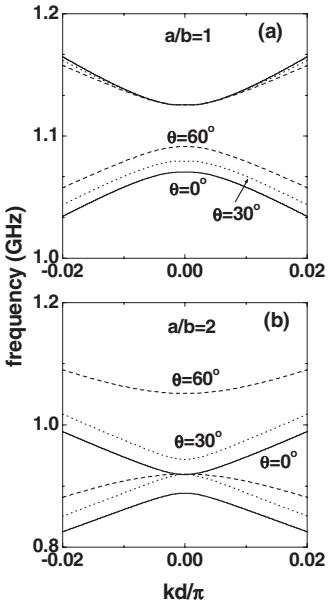

FIG. 3. Magnification of the photonic-band structure of Fig. 2 in the frequency range containing the zero-$\bar{Q}$ gaps.

We first note that, ignoring quantitative difference and some details (see Fig. 3), the results depicted in Fig. 2(a), for $a/b=1$, are very similar to those shown in Fig. 2(b) for $a/b=2$. In particular, both structures exhibit a peculiar behavior around the magnetic plasma frequency $\nu_m=\omega_m/2\pi$, which is determined by a strong coupling between the radiation field and the "magnetic plasma" contained in layer B. It is clear that this coupling is only effective for $\theta\neq 0$ and may be seen as an effect which causes a splitting, of the $\theta=0$ second band into two $\theta\neq 0$ bands. Due to this splitting, a ω_m gap (or ν_m gap) opens between these bands, which increases with θ for a given value of the ratio a/b, as shown in Figs. 2(a) and 2(b) [see also Fig. 4]. The occurrence of such a gap, for $\theta\neq 0$, is a direct consequence of the singularity in either function $r(\omega)$ in Eq. (6) or function $s(\omega)$ in Eq. (7) for $\omega=\omega_m$. It should be noted that this singularity disappears when θ tends to zero, which explains why the $\theta=0$ second band in either Fig. 2(a) or 2(b) does not exhibit the mentioned splitting. It is important to note that, when the reduced Bloch wave vector $\tau=kd/\pi$ increases from zero, the $\theta\neq 0$ second band tends rapidly to a flat function of τ (see also Fig. 6).

Note now that, as shown in Fig. 3, the dispersion curves also exhibit some interesting properties around the frequency ν_0 at which the zero-$\bar{Q}$ gap opens. In particular, it is clearly seen that the corresponding band edges depend, in general, on the propagation angle θ, for a given value of the ratio a/b. As a quantitative description of these band edges and those associated with the ω_m gap is of special importance in the understanding of the photonic-band structure, we show in Fig. 4 the explicit dependence on θ of these edges, for various values of the ratio a/b. In Fig. 4, curves r_1 and q_1 (s_m and r_2) are the edges of the zero-$\bar{Q}$ gap (ω_m gap) and correspond to the zeros of $r(\omega)$ and $q(\omega)$ [$s(\omega)$ and $r(\omega)$], respectively. In consequence, the modes associated with curves r_1 and q_1 (r_2 and s_m) have, respectively, positive and negative

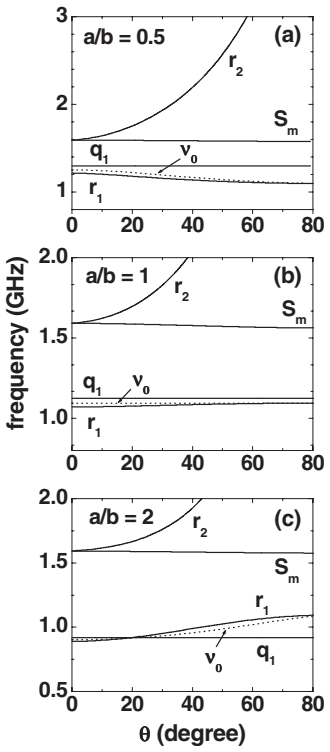

FIG. 4. Angular dependence of the frequencies $\nu=\omega/2\pi$ corresponding to the band edges for (a) $a/b=0.5$, with $a=6$ mm, (b) $a/b=1$, with $a=12$ mm, and (c) $a/b=2$, with $a=12$ mm. The dotted lines represent the frequency $\nu_0=\omega_0/2\pi$ at which $\bar{Q}=0$, curves r_1 and q_1 represent the zero-$\bar{Q}$-gap edges (at $k=0$), S_m is the top (at $k=\pm\pi/d$) of the second band, and r_2 is the bottom (at $k=0$) of the third band. The corresponding bands, for $a/b=1$ and 2, are shown in Fig. 2.

parities as functions of z. The dotted curves correspond to the frequency ν_0. With respect to the theoretical results presented in Figs. 4(a)–4(c), the following should be noted. First, in each one of them, where the ratio a/b is given, the ω_m gap exhibits a rapid increase with θ which is due to the fact that the coupling between the radiation field and the magnetic plasma contained in the structure becomes stronger. Second, for $a/b=1$, both ν_0 and the upper edge of the zero-$\bar{Q}$ gap are practically independent of θ, whereas the lower one increases with θ but cannot reach values greater than ν_0. This implies the existence of a frequency range, not centered around ν_0, where the zero-$\bar{Q}$ gap is an omnigap. A simple analysis of Fig. 4(a) leads to a similar conclusion for $a/b=0.5$. Note, however, that according to Fig. 4(c), the photonic structure, for $a/b=2$, does not possess such a type of omnigap. This is the expected result if the dependence of ν_0 on the propagation angle θ is taken into account [cf. Fig. 1(b)]. As shown in panel (c) of Fig. 4, the absence of such an omnigap is associated with a curious behavior of the zero-$\bar{Q}$-gap edges as functions of θ. In fact, we observe that when θ increases from zero, such edges approach each other with different parities, they touch each other at a given value θ_0 of θ, and then move away, interchanging their parities. Further, since the photonic bands of the considered structure may be

classified[21] according to their parities at $k=0$, this phenomenon corresponds to a band inversion phenomenon. Third, it is interesting to notice that, for $a/b=0.5$ and 1, the upper edges of the zero-$\bar{Q}$ gap are essentially flat as functions of θ, whereas the corresponding edge for $a/b=2$ is a varying function of θ. As the former edges are nearer to ν_m than the latter one, such a behavior may be understood as due to the coupling between the radiation field and the magnetic plasma mentioned above.

Furthermore, the properties of the zero-$\bar{Q}$ gap, for a given value of the propagation angle θ, are essentially the same as those established for the zero-$\bar{n}$ gap.[8] In fact, as the frequencies ν_e associated with the edges of the zero-$\bar{Q}$ gap are less than $\nu_p=\omega_p/2\pi\sqrt{\varepsilon_0}\approx 1.45$ GHz [see Fig. 4], there is a wide range of values of the layer thicknesses a and b for which the conditions $aQ_1(\nu_e)/2\ll 1$ and $bQ_2(\nu_e)/2\ll 1$ are satisfied. Under these conditions, the edges of the zero-$\bar{Q}$ gap, which are determined by the zeros of $q(\omega)$ and $r(\omega)$ [see Eqs. (5) and (6)], are only dependent on the ratio a/b (Ref. 17) for a fixed value of θ. This means that, in contrast with the Bragg gap, the zero-$\bar{Q}$ gap is insensitive to the geometrical scaling of the structure and to the structural disorder that is symmetric in the random parameters a and b. In consequence, if losses can be ignored,[22] the zero-$\bar{Q}$ gap is robust against disorder as long as the ratio $\bar{a}/\bar{b}$ is the same as that of the corresponding periodic system, where $\bar{a}$ and $\bar{b}$ are the average of the RHM and LHM layers over the structure, respectively. These unusual properties of the considered structure open up the possibility of investigating their potential use in new devices such as highly directive sources and wave front converters.

We now turn to the study of the electric fields associated with the photonic bands displayed in Fig. 2. These fields are obtained from either Eqs. (11) and (12) or (13) and (14) by substituting there the appropriate values of the geometrical and material parameters. The results of these calculations were used to present in Fig. 5 the normalized electric field intensity associated with the second and third bands (band 2 and band 3) shown in Figs. 2(a) and 2(b) as a function of the spatial distance z (in units of the lattice constant d). The variable z is limited, of course, to an elementary cell: $-a/2<z<a/2+b$. It should be pointed out that, for obvious reasons, when the edge of the considered band at $k=0$ is determined by a zero of $q(\omega)$ [$r(\omega)$], the corresponding modes along such a band are calculated by using Eqs. (13) and (14) [Eqs. (11) and (12)].

For a better description and understanding of these results, bands 2 and 3 are displayed in Fig. 6 for $a/b=1$ and $\theta=\pi/6$. The open circles correspond to the frequencies at $\tau=kd/\pi=0,0.3,0.6,0.9$ and the dotted line represents the plasma frequency $\nu_m=\omega_m/2\pi$. A similar figure is obtained for $a/b=2$. Now, some interesting features are clearly seen in Fig. 5. In fact, we observe in each one of Figs. 5(a), 5(b), and 5(d) that, when τ increases from zero, the electric field intensity, for a fixed value of the spatial distance z, increases until it reaches its maximum value at some value of τ, and then decreases. This behavior is a direct consequence of the fact that the corresponding modes at $\tau=0$ and $\tau=1$ have

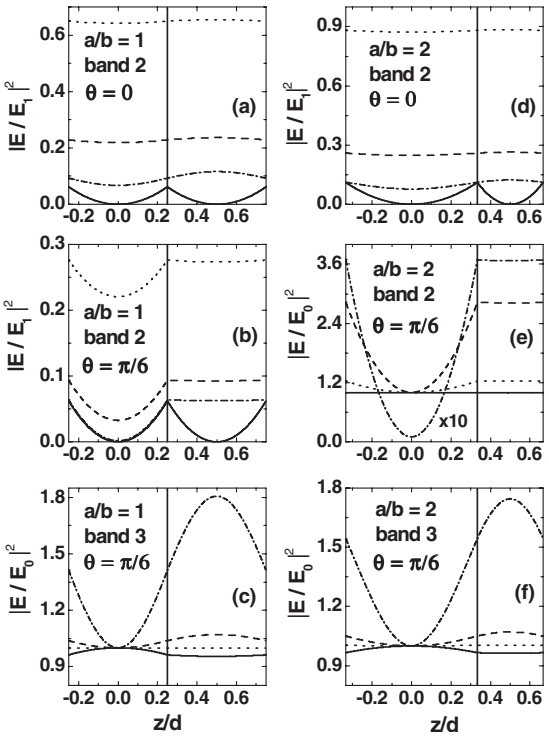

FIG. 5. z dependence (in units of the lattice constant d) of the electric field intensities associated with the second and third photonic bands (bands 2 and 3) displayed in Fig. 2, for $\theta=0$ and $\pi/6$, ratios: [(a)–(c)] $a/b=1$; [(d)–(f)] $a/b=2$, and the reduced Bloch wave vector $\tau=kd/\pi=0$ (solid lines), 0.3 (dotted lines), 0.6 (dashed lines), and 0.9 (dash-dotted lines).

negative parity. One sees also in each one of Figs. 5(c), 5(e), and 5(f) that, for a given value of $z\neq 0$, the electric field intensity is an increasing function of the reduced Bloch wave vector τ, whereas it does not vary with τ at $z=0$. It is equal to 1 at the latter point. These are the expected results if we take into account that the corresponding modes have positive and negative parities at $\tau=0$ and $\tau=1$, respectively. On the other hand, as one can see in panels (b), (c), (e), and (f) of Fig. 5, the electric field intensity associated with the $\theta=\pi/6$ photonic bands (band 2 and band 3) exhibits an inter-

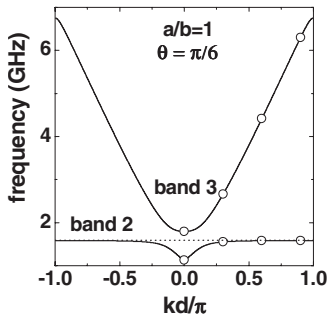

FIG. 6. Dispersion curves corresponding to the second and third bands (bands 2 and 3) of Fig. 2 for $a/b=1$ and $\theta=\pi/6$. The open circles correspond to the frequencies $\nu=\omega/2\pi$ at $\tau=kd/\pi=0$, 0.3, 0.6, and 0.9, and the dotted line represents the magnetic plasma frequency $\nu_m=\omega_m/2\pi$.

esting behavior as a function of the reduced wave vector τ, when the frequency ω of the electromagnetic field is close to the magnetic plasma frequency ω_m. In fact, near the bottom of band 3, where $\tau \lesssim 0.2$, and in that part of the spectrum where band 2 is essentially flat, i.e., for $\tau \gtrsim 0.3$, the electric field intensity is practically flat as a function of z for $a/2 < z < a/2+b$, i.e., in the region where material B is localized. A similar behavior (not shown) in such layer was found for the corresponding phase $\phi(z)$ of $E(z)$. This means that $\frac{dE(z)}{dz} \approx 0$ in such a region and therefore $E(z)$ is practically independent of z in it. This is the expected result as the electric field must satisfy Eq. (2), with $q=\frac{\omega}{c}\sin\theta$, and the magnetic permeability $\mu_2(\omega)$ of material B is small when ω is close to the magnetic plasma frequency ω_m.

Finally, in order to appreciate the importance of studying the distribution of electric field intensity in the system, let us express the energy flux associated with the corresponding modes in terms of $E(z)$. Using Eqs. (1) and (2) and the definition of the time-averaged Poynting vector, it is not difficult to see that the relation between these quantities is given by (for TE modes)

$$\vec{S} = \frac{c^2}{8\pi\mu(z)\omega}|E(z)|^2\left[\hat{x}q + \hat{z}\frac{d\phi(z)}{dz}\right], \tag{20}$$

where $\phi(z)$ is the phase of $E(z)$, i.e., $E(z)=|E(z)|\exp[i\phi(z)]$. It follows from Eq. (20) that the properties of the normal and parallel components of the Poynting vector (energy flux) are directly connected with those of the electric field intensity discussed above. Note that, in each layer, the z dependence of the parallel component S_x exhibits, for $q \neq 0$, the same structure as that of the electric field intensity, whereas the normal component S_z follows a similar behavior, but modulated by $d\phi(z)/dz$. Note, in particular, that if $d\phi(z)/dz=0$ in some region, $S_z=0$ and there is only energy flow parallel to the layers in such region. As discussed above, this latter situation occurs approximately in layer B of the considered photonic crystal when the propagation angle is different from zero and the frequency of the modes is near the magnetic plasma frequency (see Fig. 5). Thus, these observations illustrate clearly the role and significance of the electric field distribution in the study of the electromagnetic properties of the considered system.

IV. CONCLUSIONS

In this work, we have presented a detailed study of the angular dependence of the dispersion relation and associated electric fields for TE modes in 1D photonic crystals composed of alternating layers of air and a medium B with a plasmalike dispersion for both the permittivity and permeability. We have demonstrated that the photonic-band structure exhibits some interesting features around both the magnetic plasma frequency $\omega_m=2\pi\nu_m$ and the frequency $\omega_0=2\pi\nu_0$ at which $\bar{Q}=0$. Around ω_m, a band gap opens for $\theta \neq 0$ (oblique propagation) due to the occurrence of a strong coupling between the radiation field and the magnetic plasma contained in medium B. Both the higher band associated with the coupled modes and the lower one exhibit a plasmonlike behavior when ω is sufficiently close to ω_m, whereas the former band exhibits a photonlike behavior for higher frequencies. Around ω_0, a zero-$\bar{Q}$ gap opens, and its properties, as functions of the propagation angle θ, depend on the geometrical and physical parameters of the constituents. We showed that contrary to the conclusion of Jiang *et al.*,[11] the zero-$\bar{Q}$ gap is not necessarily an angle insensitive omnigap. This result confirms the conclusion of Daninthe *et al.*[12] Nevertheless, when the geometrical and physical parameters are chosen appropriately, as done by Jiang *et al.* and shown above, it is feasible to have a RHM-LHM-photonic crystal possessing such a type of omnigap. With respect to such a choice, it is very useful to take into account that, for $a/b=1$, the frequency ω_0 is independent of θ (see Fig. 1) for any RHM-LHM-photonic crystal for which the equation $n_1^2=n_2^2(\omega)$ has a real solution. Under these conditions, the existence of an angle insensitive omnigap is, in general, guaranteed. On the other hand, it was shown that, in order to understand appropriately the properties of the photonic crystals, it is necessary to have a detailed knowledge of the spatial symmetry (parities) of the modes. This allowed us to show, in particular, that the photonic-band inversion phenomenon can occur in such a structure, which can also exhibit a zero-$\bar{Q}$ gap of zero width. We stress that our analysis can be readily extended in order to treat TM modes [see comment after Eq. (3)] and any other RHM-LHM-photonic crystal of interest.

ACKNOWLEDGMENT

I would like to thank R. L. Soto Morán for critically reading the manuscript.

APPENDIX

To derive expressions (11)–(14), it is convenient to rewrite Eq. (3) as follows:

$$-\mu(z)\frac{d}{dz}\left[\frac{1}{\mu(z)}\frac{dE(z,q)}{dz}\right] = Q^2E(z,q), \tag{A1}$$

where $Q^2=(\omega^2/c^2)\mu(z)\varepsilon(z)-q^2$ and $E(z,q)$ is the electric field for a given value of q. As the physical parameters $\varepsilon(z)$ and $\mu(z)$ are constant in each layer of the photonic crystal, it follows from Eq. (A1) that if $E(z,0)$ is known in terms of such parameters, the electric field $E(z,q)$, for $q \neq 0$, can be obtained from it by performing the appropriate substitutions. This observation allows us to construct $E(z,q)$ from the formulas for $E(z,0)$ reported in Ref. 17 (second reference), which were derived by using the transfer-matrix method used in Sec. II. Now, a comparison between Eq. (4) of the mentioned reference with Eq. (A1) indicates that the appropriate substitutions are $\omega|n_1|/c \to Q_1$, $\omega|n_2|/c \to Q_2$, $Z_1n_1 \to \mu_1$, and $Z_2n_2 \to \mu_2$. It is not difficult to verify that these substitutions change Eqs. (20) and (21) of Ref. 17 (second reference) into expressions (11)–(14) for $E(z,q)$, where Q_1 and Q_2 are given in Eq. (8).

[1] D. R. Smith, W. J. Padilla, D. C. Vier, S. C. Nemat-Nasser, and S. Schultz, Phys. Rev. Lett. **84**, 4184 (2000).
[2] R. A. Shelby, D. R. Smith, S. C. Nemat-Nasser, and S. Schultz, Appl. Phys. Lett. **78**, 489 (2001).
[3] R. A. Shelby, D. R. Smith, and S. Schultz, Science **292**, 77 (2001).
[4] V. G. Veselago, Sov. Phys. Usp. **10**, 509 (1968).
[5] S. A. Ramakrishna, Rep. Prog. Phys. **68**, 449 (2005).
[6] J. B. Pendry, Phys. Rev. Lett. **85**, 3966 (2000).
[7] W. L. Barnes, A. Dereux, and T. W. Ebbesen, Nature (London) **424**, 824 (2003).
[8] J. Li, L. Zhou, C. T. Chan, and P. Sheng, Phys. Rev. Lett. **90**, 083901 (2003).
[9] L. Wu, S. He, and L. Shen, Phys. Rev. B **67**, 235103 (2003).
[10] D. Bria, B. Djafari-Rouhani, A. Akjouj, L. Dobrzynski, J. P. Vigneron, E. H. El Boudouti, and A. Nougaoui, Phys. Rev. E **69**, 066613 (2004).
[11] H. Jiang, H. Chen, H. Li, and Y. Zhang, Appl. Phys. Lett. **83**, 5386 (2003).
[12] H. Daninthe, S. Foteinopoulou, and C. M. Soukoulis, Photonics Nanostruct. Fundam. Appl. **4**, 123 (2006).
[13] N. C. Panoiu, R. M. Osgood, Jr., S. Zhang, and S. R. J. Brueck, J. Opt. Soc. Am. B **23**, 506 (2006).
[14] J. B. Pendry and D. R. Smith, Phys. Today **57**(6), 37 (2004).
[15] Y. Zhang and A Mascarenhas, Mod. Phys. Lett. B **19**, 21 (2005).
[16] M. de Dios–Leyva, J. Sabin, and J. López-Gondar, Phys. Status Solidi B **134**, 615 (1986).
[17] S. B. Cavalcanti, M. de Dios-Leyva, E. Reyes-Gómez, and L. E. Oliveira, Phys. Rev. B **74**, 153102 (2006); Phys. Rev. E **75**, 026607 (2007).
[18] R. Ruppin, Phys. Lett. A **227**, 61 (2000); J. Phys.: Condens. Matter **13**, 1811 (2001).
[19] I. V. Shadrivov, A. A. Sukhorukov, and Y. S. Kivshar, Appl. Phys. Lett. **82**, 3820 (2003).
[20] N. Engheta and R. W. Ziolkowski, IEEE Trans. Microwave Theory Tech. **53**, 1535 (2005).
[21] K. Sakoda, *Optical Properties of Photonic Crystals* (Springer, Berlin, 2001).
[22] For the considered photonic crystals, the effects of losses can be considered by including the imaginary part of $\varepsilon_2(\omega)$ and $\mu_2(\omega)$ in the calculations. In this case, condition (17) as well as the conditions for which the zero-$\bar{Q}$ gap is insensitive to the geometrical scaling cannot be satisfied and instead of a zero-$\bar{Q}$ gap another type of band gap should form. In general, the properties of the latter gap must be substantially different to those of the former one, except when the losses are relatively small (see Ref. 9).